# Exploring the Active Center of Human Acetylcholinesterase with Stereomers of an Organophosphorus Inhibitor with Two Chiral Centers†

Arie Ordentlich,‡ Dov Barak,§ Chanoch Kronman,‡ Hendrik P. Benschop,|| Leo P. A. De Jong,|| Naomi Ariel,‡ Ruth Barak,⊥ Yoffi Segall,§ Baruch Velan,‡ and Avigdor Shafferman*,‡

*Departments of Biochemistry & Molecular Biology, Organic Chemistry, and Analytical Chemistry, Israel Institute for Biological Research, Ness-Ziona 74100, Israel, and Department of Chemical Toxicology, TNO Prins Maurits Laboratory, 2280 AA Rijswijk, The Netherlands*

*Received September 21, 1998; Revised Manuscript Received December 18, 1998*

ABSTRACT: The stereoselectivity of the phosphonylation reaction and the effects of adduct configuration on the aging process were examined for human acetylcholinesterase (HuAChE) and its selected active center mutants, using the four stereomers of 1,2,2-trimethylpropyl methylphosphonofluoridate (soman). The reactivity of wild type HuAChE toward the $P_S$-soman diastereomers was $4.0-7.5 \times 10^4$-fold higher than that toward the $P_R$-diastereomers. Aging of the $P_SC_S$-somanyl−HuAChE conjugate was also $>1.6 \times 10^4$-fold faster than that of the corresponding $P_RC_S$-somanyl adduct, as shown by both reactivation and electrospray mass spectrometry (ESI/MS) experiments. On the other hand, both processes exhibited very limited sensitivity to the chirality of the alkoxy group $C_\alpha$ of either $P_S$- or $P_R$-diastereomers. These stereoselectivities presumably reflect the relative participation of the enzyme in stabilization of the Michaelis complexes and in dealkylation of the respective covalent conjugates, and therefore could be utilized for further probing of the HuAChE active center functional architecture. Reactivities of HuAChE enzymes carrying replacements at the acyl pocket (F295A, F297A, and F295L/F297V) indicate that stereoselectivity with respect to the soman phosphorus chirality depends on the structure of this binding subsite, but this stereoselectivity cannot be explained only by limitation in the capacity to accommodate the $P_R$-diastereomers. In addition, these acyl pocket enzyme mutants display some (5−10-fold) preference for the $P_RC_R$-soman over the $P_RC_S$-stereomer, while reactivity of the hydrophobic pocket mutant enzyme W86F toward the $P_RC_S$-soman resembles that of the wild type HuAChE. Residue substitutions in the H-bond network (E202Q, E450A, Y133F, and Y133A) and the hydrophobic pocket (F338A, W86A, W86F, and Y337A) result in a limited stereoselectivity for the $P_SC_S$- over the $P_SC_R$-stereomer. Aging of the $P_S$-somanyl conjugates with all the HuAChE mutant enzymes tested practically lacked stereoselectivity with respect to the $C_\alpha$ of the alkoxy moiety. Thus, the inherent asymmetry of the active center does not seem to affect the rate-determining step of the dealkylation process, possibly because both the $P_SC_S$- and the $P_SC_R$-somanyl moieties yield the same carbocationic intermediate.

Acetylcholinesterase (AChE,[1] EC 3.1.1.7) is among the most efficient enzymes, with a turnover number of $>10^4$ $s^{-1}$ (*1*). While the mechanistic and structural origins of its catalytic power and high reactivity toward organophosphorus inhibitors have been a subject of interest for several decades, only recent studies have begun to delineate the unique functional architecture of the AChE active center. These include X-ray crystallography (*2*−*5*), site-directed mutagenesis, and molecular modeling together with kinetic studies of the AChE mutants with substrates and reversible inhibitors (*6*−*14*). The functional roles of the various active center subsites, charted this way, in the reactivity characteristics of the enzyme include (a) the esteratic site containing the active site serine, (b) the "oxyanion hole" consisting of residues Gly121*(118)*,[2] Gly122*(119)*, and Ala204*(201)*, (c) the "anionic subsite" or the choline binding subsite, Trp86*(84)*, (d) the hydrophobic site for the alkoxy leaving group of the substrate containing an "aromatic patch" that includes residues Trp86*(84)*, Tyr337*(330)*, and Phe338*(331)*, and (e) the acyl pocket, Phe295*(288)* and Phe297*(290)*. In butyryl-

† This work was supported by the U.S. Army Research and Development Command (Contract DAMD17-96-C-6088) and by the Directorate of Military Medical Sciences of the Ministry of Defence, The Netherlands.

* To whom correspondence should be addressed: Israel Institute for Biological Research, Ness-Ziona 74100, Israel. Telephone: (972)-8-9381518. Fax: (972)-8-9401404. E-mail: avigdor@iibr.gov.il.

‡ Department of Biochemistry & Molecular Biology, Israel Institute for Biological Research.

§ Department of Organic Chemistry, Israel Institute for Biological Research.

|| Department of Analytical Chemistry, Israel Institute for Biological Research.

⊥ TNO Prins Maurits Laboratory.

[1] Abbreviations: AChE, acetylcholinesterase; HuAChE, human acetylcholinesterase; TcAChE, *Torpedo californica* acetylcholinesterase; BoAChE, bovine acetylcholinesterase; BChE, butyrylcholinesterase; EqBChE, equine butyrylcholinesterase; ATC, acetylthiocholine; BTC, butyrylthiocholine; soman, 1,2,2-trimethylpropyl methylphosphonofluoridate; DFP, diisopropyl phosphorofluoridate; DEFP, diethyl phosphorofluoridate; paraoxon, *p*-nitrophenyl diethyl phosphate.

[2] Amino acids and numbers refer to HuAChE, and the numbers in parentheses refer to the positions of analogous residues in TcAChE according to the recommended nomenclature (*50*).

10.1021/bi982261f CCC: $18.00 
Published on Web 02/18/1999

Scheme 1

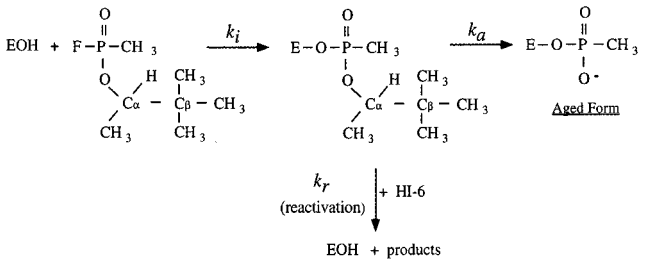


cholinesterase (BChE), which unlike AChE can catalyze efficiently hydrolysis of larger molecules such as butyryl-, benzoyl-, or succinylcholine, the modified substrate selectivity was shown to result mainly from differences in the acyl pocket structure between the two enzymes (*6*, *9*, *15*).

For further exploration of the functional architecture of the AChE active center, it is necessary to use specific ligands that probe the various facets of the enzyme reactivity. AChE organophosphorus inhibitors seem to be particularly suitable for this task since their unusually high reactivity toward the enzyme suggests an efficient accommodation by the active center binding elements (*12*, *15*−*17*). Their ground-state tetrahedral geometry, compared to that of the planar substrates, affords an additional dimension for mapping the spacial organization of these binding elements (*12*, *15*). In addition, AChE reactions with organophosphonates display marked stereoselectivity (*15*−*17*) which can also be utilized for investigation of the hydrophobic and steric interactions with the structural elements of the active center. Soman is a prime example of such AChE inhibitors, combining an outstanding phosphylating[3] activity with chiral preference in the range of 4 orders of magnitude in favor of the $P_S$-diastereomers (*18*, *19*). In addition, interactions with soman may be modulated by additional subsites in the AChE active center, due to the chiral $C_\alpha$ (see Scheme 1) of the inhibitor's alkoxy moiety (interactions of the four soman stereomers with HuAChE are displayed in Figure 1). Indeed, recent studies with certain BChE mutants demonstrated substantial stereoselectivity toward the $P_SC_S$-soman stereomer (*20*), indicating that differential reactivity of the $P_S$-diastereomers may assist in probing the fine structure of the AChE hydrophobic pocket.

Due to the tetrahedral geometry of the phosphonate inhibitor in the initial Michaelis complex as well as in the covalent conjugate, and the limited motion of the equatorial phosphorus substituents in the pentacoordinate transition of the nucleophilic addition, the phosphonyl moiety in both adducts may face similar regions of the active center structural manifold. As a result, the same interactions that govern the stability of the initial complex may be also important in facilitating a characteristic chemical transformation of the covalent somanyl−AChE conjugate, the aging process (*21*, *22*). Thus, the relative rates of phosphonylation by soman stereomers, as well as those of the postinhibitory processes (aging, see Scheme 1) for the stereomeric soman conjugates, may provide another sensitive measure for probing the effects of structural perturbations at the phosphonyl binding locus of HuAChE (for related studies, see refs *12*, *15*, and *22*).

[3] The comprehensive term "phosphyl" is adopted from Bourne and Williams (*51*) for all tetravalent phosphorus electrophilic groups.

In this study, we further explore (*23*, *24*) the functional architecture of the HuAChE active center, using enzymes that carry residue substitutions at the various active center subsites, and examine the effects of structural perturbations on the reactivity and stereoselectivity of the resulting mutants with respect to the soman stereomers. We find that the pronounced HuAChE stereoselectivity with respect to the phosphorus chirality cannot be explained solely by steric interference at the acyl pocket. We find also, in accordance with the previously described mechanism of aging, that the dealkylation process of the various somanyl−HuAChE conjugates is not stereoselective with respect to chirality of the phosphonyl alkoxy substituent.

## MATERIALS AND METHODS

*Enzymes and Reagents.* Expression of recombinant HuAChE and its mutants in a human embryonal kidney-derived cell line (HEK-293) (*8*, *25*, *26*) and generation of all the mutants were described previously (*6*, *8*, *21*, *27*, *28*). Stable recombinant cell clones expressing high levels of each of the mutants were established according to the procedure described previously (*25*). Enzymes were purified (>90% pure) either by ligand affinity chromatography (*25*) or by fractionation on a monoclonal antibody affinity column (*6*). The monomeric C580S HuAChE enzyme, expressed in *Escherichia coli* with an N-terminus sequence Met-Glu-Gly-Arg, was a gift from M. Fischer (*29*). EqBChE was purified using a modification of the ligand affinity chromatographic method described previously (*25*). Acetylthiocholine iodide (ATC), 5,5′-dithiobis(2-nitrobenzoic acid) (DTNB), and 1-(2-hydroxyiminomethylpyridinium)-1-(4-carboxyiminopyridinium) dimethyl ether dichloride (HI-6) were purchased from Sigma. Preparation of diastereomeric mixtures of the $C_S$- and $C_R$-1,2,2-trimethylpropyl methylphosphonofluoridates (soman) followed an accepted synthetic procedure using methylphosphonodifluoride (*30*) and the appropriate optically pure pinacolyl alcohol (*19*). The pure diastereomers of $P_S$- and $P_R$-soman (for provisional assignment of absolute configuration with respect to the phosphorus, see the Results) were isolated from incubations with rabbit serum or α-chymotrypsin, respectively, as described previously (*19*). Since samples of the $P_RC_S$- and $P_RC_R$-soman, obtained in this manner, contained up to 4% of the corresponding $P_S$-diastereomer (as determined by $^{31}P$ NMR and by titration with wild type HuAChE), they were further purified by reincubaton with α-chymotrypsin. The resulting $P_R$-soman diastereomers were >99% optically pure, according to HuAChE titration with a $>10^3$-fold higher concentration of the inhibitor. Purified $P_R$-soman diastereomers were stored in dry acetonitrile at −20 °C.

*Measurements of Enzyme Activity and Phosphonylation Rates.* HuAChE activity was assayed according to Ellman et al. (*31*) [in the presence of 0.1 mg/mL BSA, 0.3 mM DTNB, 50 mM sodium phosphate buffer (pH 8.0), and various concentrations of ATC], in experiments carried out at 27 °C, and monitored by a Thermomax microplate reader (Molecular Devices). Measurements of phosphonylation rates of the HuAChE enzymes, by the $P_S$-soman diastereomers, were carried out essentially as described previously for reactions with racemic soman, using four to six different concentrations of $P_SC_S$- or $P_SC_R$-soman (*I*) and monitoring

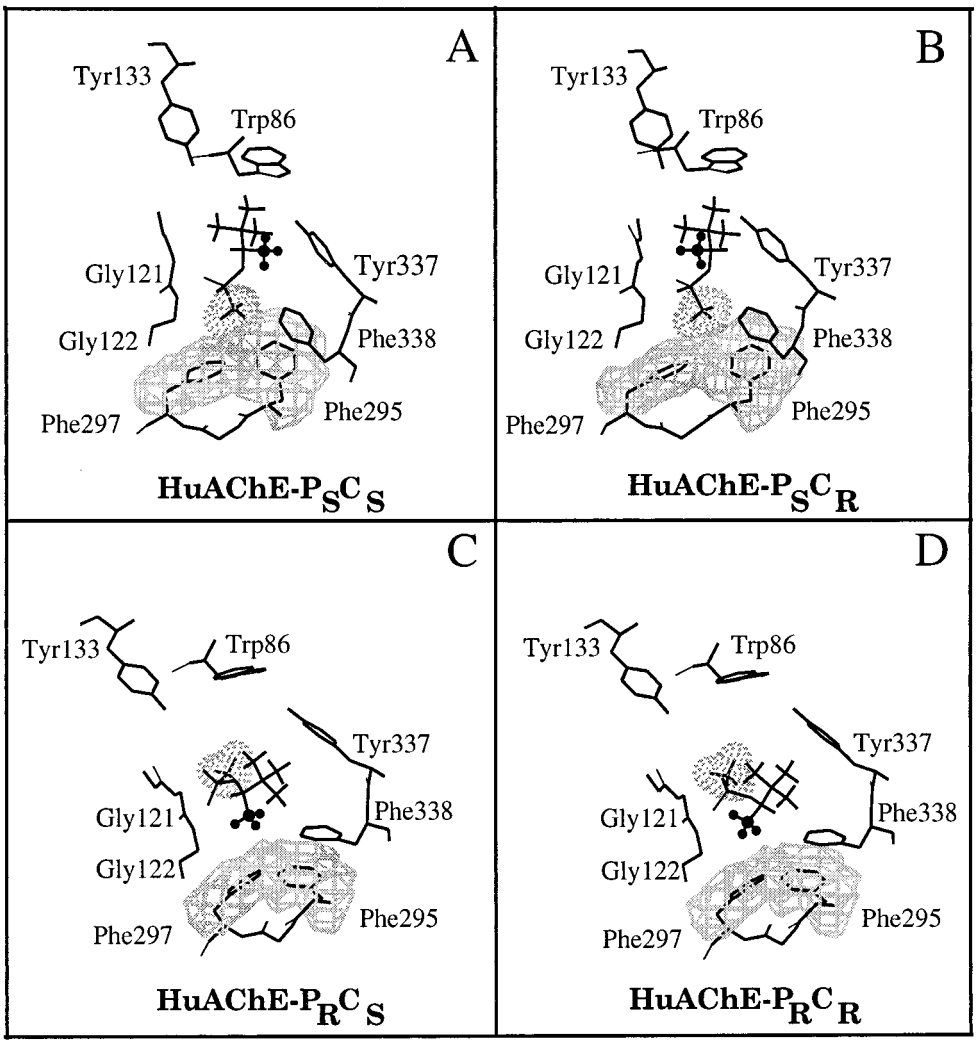


FIGURE 1: Michaelis complexes of HuAChE with soman stereomers. Inhibitor configurations are shown in each panel. Only amino acids adjacent to the inhibitor are shown, while hydrogen atoms of the protein are omitted for clarity. The soman $C_\alpha$-methyl substituent is displayed as balls and sticks. Molecular volumes of the phosphorus methyl substituent and of the aromatic moieties of residues Phe295 and Phe297 are shown with dots and grids, respectively. For the $P_S$-soman−HuAChE complexes, the fit of the phosphorus methyl substituent with residues of the acyl pocket and the different positioning of the $C_\alpha$-methyl substituent relative to the aryl moiety of residue Tyr337 are shown in panels A and B. Note that in the $P_R$-soman−HuAChE complexes (panels C and D) the acyl pocket cannot accommodate the bulky *tert*-butyl portion of the $P_R$-soman alkoxy moiety and it points away from the phenyl groups defining this acyl pocket (for the three-dimensional orientation, see Figure 3A).

the enzyme residual activity ($E$) at various times. The apparent bimolecular phosphonylation rate constants ($k_i$) determined under pseudo-first-order conditions were computed from the plot of slopes of ln($E$) versus time at different inhibitor concentrations. Rate constants under second-order conditions were determined from plots of $\ln\{E/[I_o - (E_o - E)]\}$ versus time (*23*).

Phosphonylation rate constants of HuAChE enzymes by the $P_R$-soman diastereomers were determined under second-order conditions using phosphonate and enzyme concentrations in the range of $10^{-5}$−$10^{-6}$ M. Reactions were carried out in 50 mM Tris buffer to minimize the effects of phosphonate racemization (*19*) and were followed for periods not exceeding two half-lifes.

*Measurements of Aging Rates.* The initial soman-inhibited enzymes were obtained under conditions where the rate of phosphonylation is much faster than the rate of aging [$k_i(I_o) \gg k_a$] and with over 98% inhibition of the initial enzyme activity. The excess soman was rapidly removed either by column filtration (Sephadex G-15) or by 1000-fold dilution, prior to reactivation. The reactivatable (nonaged soman conjugate) fraction was assessed by reactivation with 0.5 mM HI-6 under conditions where the rate of reactivation is faster than the rate of aging ($k_r$[HI-6] > $k_a$; see Scheme 1). The activity of the reactivated enzyme ($E_r$) was routinely corrected for the inhibitory effect of the reactivator (*32*). The first-order rate constants of aging ($k_a$) were determined from the slopes of ln($E_r$) versus time.

*Mass Spectrometric Analysis.* Molecular mass measurements were carried out on a VG Platform mass spectrometer, which consists essentially of an electrospray ion source operating at atmospheric pressure followed by a quadrupole mass analyzer. Samples of diastereomeric somanyl−HuAChE conjugates, prepared by mixing the enzyme (30−40 pmol/$\mu$L) with an excess of the appropriate phosphonofluoridate in deionized water (pH ~6.5), were assayed as described previously (*33*). The multiply charged electrospray ionization mass spectra were converted to the true molecular mass spectra using the VG MaxEnt algorithm of the MassLynx NT software. Molecular mass calculations of

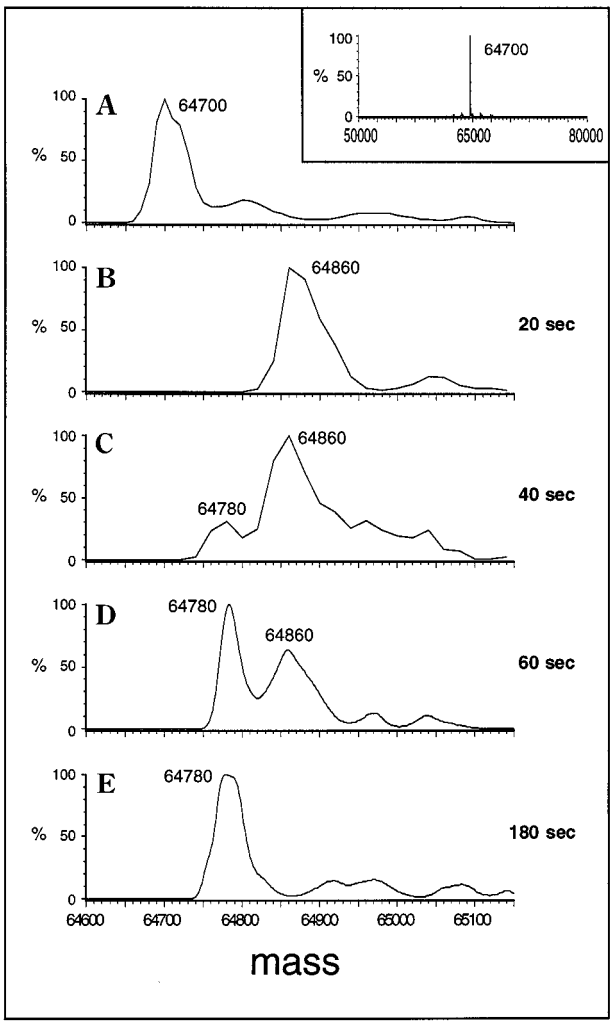


FIGURE 2: Progression of the aging reaction of $C_S$-somanyl−HuAChE monitored by positive-ion ESI-MS. Molecular masses of the mixture components were obtained for each spectrum after processing by the VG MaxEnt software over a mass range of 64000−68000 Da. (A) Free C580S HuAChE from a bacterial source (mass calculated from sequence of 64 695 Da). The same sample calculated over a wider mass range (50000−80000 Da) is shown in the inset. (B−E) Mass spectra of the reaction mixtures determined at the indicated time interval after reaction onset (at pH ~6.5) and containing varying proportions of a molecular species presumably corresponding to the $P_SC_S$-somanyl−HuAChE conjugate (calculated mass of 64 863 Da) and to the corresponding dealkylation product (calculated mass of 64 778 Da). The absence of other peaks in the spectra taken after 40 and 60 s suggests a direct transition from the species with a molecular mass of 64 860 Da to one with a molecular mass of 64 780 Da.

homogeneous samples were carried out over a mass range of 50000−80000 Da (see the inset of Figure 2).

The process of dealkylation of $P_S$-somanyl−HuAChE conjugates could be monitored by mixing aliquots from an appropriate phosphonylation mixture (20 $\mu$L) with formic acid (1 $\mu$L) followed by immediate mass spectrometric analysis using a mass range of 64000−66000 Da (Figure 2).

*Molecular Modeling.* Building and optimization of three-dimensional models of 1,2,2-trimethylpropyl methylphosphono−HuAChE conjugates were performed on a Silicon Graphics IRIS 70/GT workstation using SYBYL modeling software (Tripos Inc.). The initial models of the Michaelis complexes and of the covalent conjugates were constructed as described previously (*12*, *34*). The models were optimized by molecular mechanics using the MAXMIN force field (and AMBER charge parameters for the enzyme) and zone refined, including 127 amino acids (15 Å substructure sphere around $O^{\gamma}$-Ser203). Optimization of the initial models included restriction of the distances between the phosphonyl oxygen and the amide nitrogen atoms of residues Gly121 and Gly122 which were relieved in the subsequent refinement.

Modeling of the acyl pocket region in the $P_RC_S$-somanyl−HuAChE covalent adduct was based upon the recently resolved X-ray structure of the aged DFP−TcAChE conjugate (*35*). The conformational distortion of the main chain in the acyl pocket region was introduced into the HuAChE conjugate by manipulation of the appropriate torsion angles followed by energy optimization.

## RESULTS

*Formation and Aging of Stereomeric Soman−HuAChE Conjugates.* To use the four soman stereomers as steric probes of the HuAChE active center (see Figure 1), it is necessary to assign absolute configurations to their chiral atoms and to ascertain that the diastereomeric purity of the sample does not change during the reaction. In the case of soman, the chirality of the $C_\alpha$ is known [from the synthetic precursor 1,2,2-trimethylpropyl alcohol; $C_{(-)} = C_R$, $C_{(+)} = C_S$], while that of the asymmetric phosphorus can be provisionally assigned from chemical correlation with analogous solved structures (*36*) and from the chiroptical properties of the parent phosphonate *O*-methyl methylphosphonofluoridate (*37*) [$P_{(-)} = P_S$, $P_{(+)} = P_R$]. Fluoride-catalyzed racemization at the phosphorus could lead, during the relatively slow phosphonylations by the $P_R$-diastereomers, to their contamination by the highly reactive $P_S$-stereomers (*19*). Minimization of the extent of such racemization (see Materials and Methods), together with the extensive purification of the $P_R$-diastereomers, enabled us to determine their actual reactivity with respect to HuAChE.

Comparison of the apparent bimolecular rate constants ($k_i$) of HuAChE phosphonylation by the four stereomers of soman shows an outstanding stereoselectivity with respect to the $P_S$-diastereomers ($7.5 \times 10^4$-fold for the $P_SC_S$-stereomer over the $P_RC_S$-isomer and $4.0 \times 10^4$-fold for the $P_SC_R$-stereomer over the $P_RC_R$-isomer; see Table 1). Such AChE stereoselectivity is much higher than that observed with respect to phosphonates carrying other leaving groups such as *p*-nitrophenol (*38*) or thiocholine (*15*, *22*). These different stereoselectivities result mainly from the lower reactivity of the $P_R$-diastereomers. Thus, while the AChE phosponylation rate constant for phosphonylation by $P_S$-cycloheptylmethylphosphonylthiocholine ($1.9 \times 10^8$ min$^{-1}$ M$^{-1}$; see ref *15*) is similar to those measured for the corresponding diastereomers of soman ($1.5 \times 10^8$ and $0.8 \times 10^8$ min$^{-1}$ M$^{-1}$; see Table 1), the constant for the $P_R$-cycloheptylmethylphosphonylthiocholine ($81 \times 10^4$ min$^{-1}$ M$^{-1}$; see ref *15*) is about 400-fold higher than those for the $P_RC_S$- or the $P_RC_R$-soman isomers ($0.2 \times 10^4$ min$^{-1}$ M$^{-1}$ for both cases). The low reactivity of the $P_R$-soman isomers was already suggested in the past (see Table 1); however, due to technical limitations, the precise values of $k_i$ could not be obtained. In this study, the actual measurement of these

Table 1: Rate Constants of Phosphonylation ($k_i$) and Aging ($k_a$) of Different AChEs by Stereomers of Soman

| | | $k_i$ ($\times 10^4$ min$^{-1}$ M$^{-1}$) | | | |
|---|---|---|---|---|---|
| | | $P_SC_S$ | $P_SC_R$ | $P_RC_S$ | $P_RC_R$ |
| phosphonylation | rHuAChE[a] | 15000 ± 3000 | 8000 ± 400 | 0.2 ± 0.1 | 0.2 ± 0.1 |
| | BoAChE[b] | 18000 ± 1000 | 2700 ± 100 | <1.0 | <1.0 |
| | EelAChE[b] | 28000 ± 2000 | 18000 ± 1000 | <0.5 | <0.5 |
| | | $k_a$ ($\times 10^{-3}$ min$^{-1}$) | | | |
| | | $P_SC_S$ | $P_SC_R$ | $P_RC_S$ | $P_RC_R$ |
| aging | rHuAChE[a] | 130 ± 30 | 90 ± 30 | <0.008[d] | <0.08[e] |
| | BoAChE[c] | 74 | 82 | − | − |

[a] pH 8.0 and 24 °C. [b] pH 7.7 and 25 °C (*19*). [c] pH 7.5 and 25 °C (*18*). [d] Samples were followed for 70 days. [e] Samples were followed for 7 days.

constants was made possible by preparation of optically pure samples of the $P_R$-soman diastereomers (see Materials and Methods) and by the ability to produce sufficient amounts of recombinant HuAChE proteins, using the remarkably efficient HEK 293 expression system (*8*, *25*). Notably, for reactions of the wild type enzyme or its mutant derivatives with the $P_RC_S$-soman, enzyme concentrations of up to $5 \times 10^{-5}$ M (~3 mg/mL) were required for determination of kinetic parameters, while the corresponding concentrations used for reactions with the $P_S$-soman isomers were lower by at least 4 orders of magnitude.

In contrast to the pronounced HuAChE stereoselectivity with respect to phosphorus chirality, rates of phosphonylation by either the $P_S$- or $P_R$-soman diastereomers show negligible effect due to the chiral $C_\alpha$ of the 1,2,2-trimethylpropyloxy soman substituent (see Table 1). Such limited stereoselectivity for the $P_SC_S$-soman over the corresponding $P_SC_R$-stereomer was also reported for AChE from electric eel or BoAChE (*19*), indicating that the AChE active center environment is nearly symmetrical with respect to the $C_\alpha$ methyl substituent of the $P_S$-soman stereomers (Figure 1A,B). Our kinetic findings demonstrate now that this is true also for the $P_R$-stereomers, despite the different orientation of the alkoxy moieties of the $P_S$- and $P_R$-soman diastereomers in the active center (see models in Figures 1 and 3A).

Unlike the stereoselectivity of the phosphonylation reaction, which probably depends on specific interactions in the noncovalent Michaelis complex (see the Discussion), the stereospecificity of aging should have probed the asymmetry of the chiral soman−HuAChE covalent adducts. Yet, as already observed for the $P_S$-diastereomeric adducts of BoAChE (*18*), the rates of aging for the corresponding conjugates of HuAChE are practically equivalent (see Table 1), indicating that no specific interactions with the $C_\alpha$-methyl group are required during the dealkylation process. Similar results were recently reported for aging reactions, carried out at 4 °C and over a wide range of pH values (*39*), involving eel AChE and BoAChE (from fetal serum). The fact that the exact position of the $C_\alpha$ methyl substituent does not affect the rate of aging is consistent with a dealkylation mechanism in which the elimination proceeds via formation of a formally planar carbocation (*23*, *24*, *40*) since the same species is expected from both the $P_SC_S$- and $P_SC_R$-somanyl conjugates.

Progression of the dealkylation process could be determined directly, through monitoring of the changes in the somanyl−HuAChE conjugate molecular mass by electrospray mass spectrometry (ESI-MS; see ref *33*). For these measurements, recombinant HuAChE expressed in bacteria was used (*29*) since with such an enzyme we could avoid the extensive molecular heterogeneity due to glycosylation (*33*). The ESI-MS analysis indicates the involvement of only two molecular species in the aging reaction: the original somanyl−HuAChE conjugate and the dealkylation product. Examination of Figure 2 shows that the molecular mass of 64 860 Da, corresponding to the somanyl−HuAChE conjugate (*33*), gradually disappears and is replaced (within less than 180 s) by a molecular mass of 64 780 Da which corresponds to the aged conjugate. These results demonstrate that the time frame of the observed changes is similar to the measured value of $\tau_{1/2}$ (0.4 min at pH 6) for the corresponding aging process, as determined by monitoring the reactivability of the conjugate (*23*). Using the ESI-MS technique, it was also possible to show that the molecular masses of the $P_R$-somanyl−HuAChE conjugates did not change for a long period of time (up to 7 days), corroborating the results of reactivation experiments (see Table 1) and extending earlier observations (*18*) with regard to the resistance of these stereomeric adducts to aging. For the $P_RC_S$-somanyl−HuAChE conjugate, the reactivability was monitored for up to 70 days by incubating the adduct solution in a thermostated heatcube at 37 °C. Throughout this prolonged incubation period, full enzymatic activity could be restored by reaction of the soman−HuAChE conjugates with HI-6 (*23*). It is worth noting that samples of the free enzyme, incubated under the same conditions, are somewhat less thermostable than the soman conjugates.

*Formation of Stereomeric Soman Conjugates with HuAChE Enzymes Mutated at the Acyl Pocket*. The aromatic moieties of residues Phe295 and Phe297, in the HuAChE active center, form the binding subsite accommodating the methyl group of the substrate acyl moiety (*6*). As shown in the past, by others and us, replacements of these residues with an aliphatic amino acid (alanine, leucine, and valine) alters the substrate specificity of the mutant AChEs (*6*, *9*, *15*). Some of these mutations generated enzymes which resemble the BChE catalytic activity, hydrolyzing effectively butyrylthiocholine (BTC) as well as acetylthiocholine (ATC) (*6*, *15*). Molecular models of these modified acyl pockets suggested that the altered substrate specificity is mainly due to a better accommodation of the larger acyl moieties of butyryl- or benzoylcholines (*6*, *34*, *41*). Indeed, the increased reactivities of the AChE acyl pocket mutants F295A, F295L, F297A, and F297V as well as of the double mutant F295L/F297V toward certain phosphates seem to be mainly a consequence of removing steric restrictions on the size of

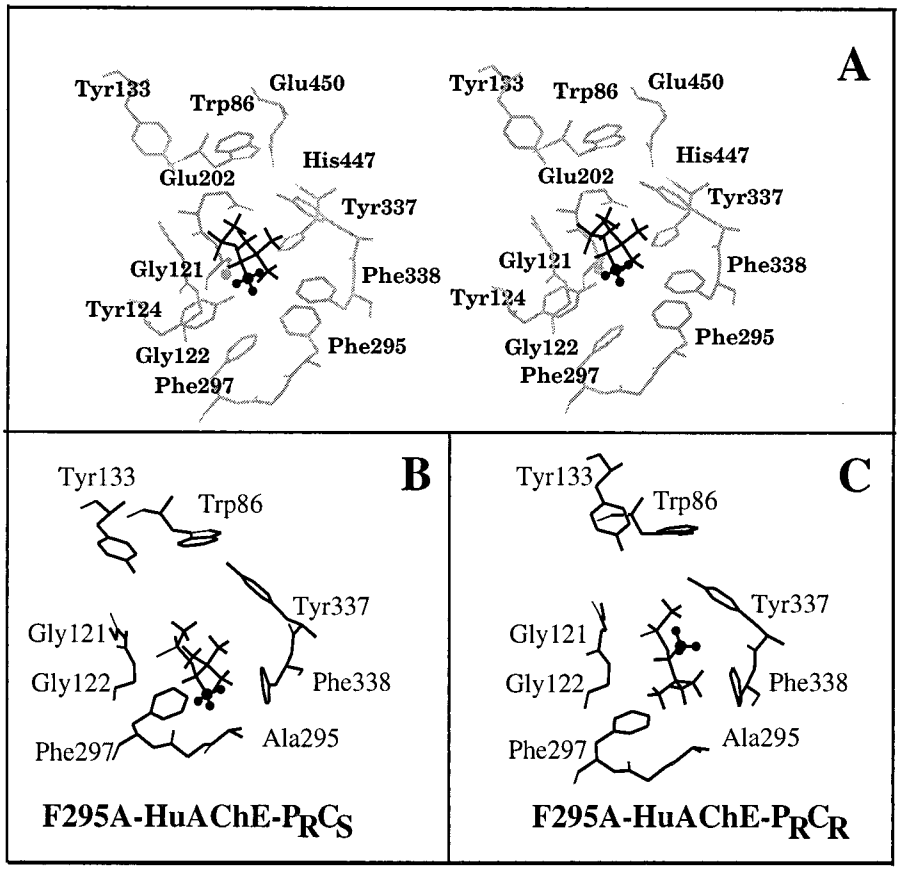


FIGURE 3: Michaelis complexes of the $P_R$-soman diastereomers with the wild type and F295A HuAChEs. Only amino acids adjacent to the inhibitor are shown, and hydrogen atoms of the protein are omitted for clarity. (A) Stereoview of the $P_RC_S$-soman−HuAChE complex exemplifying the exclusion of the soman alkoxy group from the acyl pocket and its position pointing toward the gorge exit. The inhibitor is shown as a heavy line. (B) $P_RC_S$-soman−F295A HuAChE complex. Note the ligand conformation which is analogous to that in the corresponding complex with wild type HuAChE (Figure 1C). **(**C) $P_RC_R$-soman−F295A HuAChE complex. In this case, the soman alkoxy group is partially accommodated in the acyl pocket, unlike its conformation in the complex with the wild type HuAChE (Figure 1D) or in the analogous $P_RC_S$-soman−F295A HuAChE complex (panel B).

Table 2: Rate Constants of Phosphonylation ($k_i$) of HuAChE Enzymes Mutated at the Acyl Pocket by Stereomers of Soman

| | $k_{app}$ ($\times 10^8$ $min^{-1}$ $M^{-1}$) | | $k_i$[b] ($\times 10^4$ $min^{-1}$ $M^{-1}$) | | | | stereoselectivity[c] | | | |
|---|---|---|---|---|---|---|---|---|---|---|
| | | | | | | | carbon | | phosphorus | |
| | ATC | BTC | $P_SC_S$ | $P_SC_R$ | $P_RC_S$ | $P_RC_R$ | $P_SC_S/P_SC_R$ | $P_RC_S/P_RC_R$ | $P_SC_S/P_RC_S$ | $P_SC_R/P_RC_R$ |
| rHuAChE | 28.6[a] | 0.3[a] | 15000 ± 3000 | 8000 ± 400 | 0.2 ± 0.1 | 0.2 ± 0.1 | 1.9 | 1.0 | 75000 | 40000 |
| F295A | 29.2[a] | 33.3[a] | 2000 ± 400 | 340 ± 30 | 0.2 ± 0.1 | 1.7 ± 0.2 | 5.9 | 0.1 | 10000 | 200 |
| F297A | 2.2[a] | 1.4[a] | 5000 ± 1000 | 1600 ± 200 | 0.05 ± 0.01 | 0.5 ± 0.1 | 3.1 | 0.1 | 100000 | 3200 |
| F295L/F297V | 2.2[a] | 14.0[a] | 330 ± 20 | 150 ± 70 | 1.0 ± 0.2 | 4.5 ± 0.7 | 2.2 | 0.2 | 330 | 33 |
| Y337A | 7.7[a] | 0.1[a] | 2500 ± 400 | 800 ± 100 | ≤0.04 | ND | 3.1 | − | − | − |
| Y337F | 18.5[a] | 0.9[a] | 4900 ± 300 | 1900 ± 400 | ND | ND | 2.6 | − | − | − |
| EqBChE | 1.6 | 3.0 | 6000 ± 400 | 1000 ± 300 | 12 ± 4 | 170 ± 20 | 6.0 | 0.07 | 500 | 5.9 |
| HuBChE[d] | ND | 10.0 | 4000 ± 500 | 500 ± 100 | ND | 600 ± 200 | 8.0 | − | − | 0.8 |

[a] Ordentlich et al. (*6*). [b] pH 8.0 and 24 °C. [c] Relative $k_i$. [d] pH 7.5 and 25 °C (*20*).

the acyl pocket (*12*). The modeling studies (*34*) also suggested that similar steric features of the acyl pocket in BChE may be the principal reason for its lack of stereoselectivity with respect to phosphonates such as 2-propyl methylphosphonofluoridate (sarin) (*38*).

Surprisingly, and in contrast to the above-mentioned observations, the phosphonylation rate constants of both the F295A and F297A HuAChEs by the $P_RC_S$-soman were similar or even somewhat lower than the corresponding value for the wild type enzyme (see Table 2). Thus, these modifications of the acyl pocket are apparently insufficient for improving accommodation of the bulky 1,2,2-trimethylpropyloxy moiety of the $P_RC_S$-stereomer. This inferior accommodation of the alkoxy group could be expected from the molecular models of the corresponding Michaelis complexes (Figure 3A,B) which indicate that removal of either residue Phe295 or Phe297 does not create sufficient space in the acyl pocket to fit the *tert*-butyl portion of the $P_RC_S$-soman alkoxy group. Consequently, conformations of this stereomer in noncovalent complexes with the F295A and F297A enzymes resemble those of the $P_R$-soman diastereomers in complexes of the wild type HuAChE.

Unlike the case of the $P_RC_S$-stereomer, the $P_RC_R$-soman seems to be better accommodated in the Michaelis complexes

with the F295A or F297A enzymes than with the wild type HuAChE (see Table 2). Also, for both of these mutant enzymes, the reactivity toward this stereomer is 8−10-fold higher than toward the $P_RC_S$-stereomer. This stereoselectivity is compatible with molecular models of the $P_RC_R$-soman complexes with the F295A and F297A enzymes, which show that the alkoxy moiety is partially accommodated in the acyl pocket, in contrast to its positioning in the corresponding models of the $P_RC_S$-soman (see Figure 3C). In fact, the juxtaposition of the alkoxy group with the acyl pocket in these $P_RC_R$-soman complexes seems to be similar to that modeled in the respective BChE complex (model not shown).

The reactivity of the $P_SC_S$-soman toward the F295A and F297A enzymes is also diminished (3−7-fold relative to that of the wild type enzyme), probably due to perturbation of the optimal pocket dimensions for the phosphorus methyl substituent. Similarly, the phosphonylation rate constant of the F297A HuAChE, for phosphonylation by the $P_SC_R$-soman, is 5-fold lower than the corresponding value of the wild type enzyme. On the other hand, the reactivity of this stereomer toward the F295A HuAChE is 23-fold lower relative to that of the wild type HuAChE, indicating that in this case additional enzyme−soman interactions may be affected. Due to the decreased reactivity of both the $P_SC_S$- and $P_RC_S$-soman diastereomers toward either F295A or F297A enzymes, their stereoselectivities with regard to phosphorus chirality appear to be not very different from that of the wild type HuAChE (see Table 2). In the case of the $C_S$-diastereomers, we note that the reduced stereoselectivity ($P_SC_R$ over $P_RC_R$) of the F295A enzyme, relative to that of the wild type HuAChE (200-fold compared to $4 \times 10^4$-fold, respectively), is only partially due to enhanced reactivity toward the $P_RC_R$-soman (9-fold greater than that of the wild type HuAChE). The other contribution to this stereoselectivity ($P_SC_R$ over $P_RC_R$) is a consequence of the decreased reactivity of the F295A enzyme toward the $P_SC_R$-soman (23-fold; see Table 2).

The decline of reactivity toward the $P_S$-soman diastereomers, due to replacement of either of the residues at the acyl pocket, is further demonstrated by the double mutant F295L/F297V HuAChE. Although this enzyme resembles BChE, with respect to the composition of the acyl pocket and the enhanced catalytic activity toward BTC (Table 2), its reactivity toward soman stereomers is rather different from that of BChEs. The phosphonylation rate constant of the F295L/F297V HuAChE by the $P_SC_S$-soman is about 12−18-fold lower than that for the human or equine BChE (Table 2). On the other hand, the reactivity of the double mutant toward the $P_SC_R$-soman is only 3−7-fold lower than that of the BChEs. Thus, while accommodation of both $P_S$-soman diastereomers is similarly affected by the double replacement in HuAChE, the reactivities of BChE toward these diastereomers vary, indicating that despite the "equivalence" in their acyl pockets the active center architectures of the two enzymes are quite different. Furthermore, although the bimolecular rate constant of the reaction of F295L/F297V HuAChE with the $P_RC_R$-isomer is 22-fold higher relative to that of the wild type enzyme, this rate is still 38-fold lower than that of the equine BChE with the same stereomer. This further underscores the difference in interaction of the 1,2,2-trimethylpropyloxy group with the acyl pockets of the two enzymes. In addition, the stereoselectivity of the F295L/F297V HuAChE toward the $P_SC_S$-soman stereomer over the $P_RC_S$-stereomer is comparable to that of equine BChE (330- and 500-fold, respectively); however, one should note that the reactivity toward both the $P_SC_R$- and $P_SC_S$-soman stereomers is higher (7−18-fold) in the case of equine BChE than in the case of the F295L/F297V enzyme (see Table 2).

Another difference between the active centers of HuAChE and BChE is that the position equivalent to 337 in HuAChE is occupied, in BChE, by alanine rather than by tyrosine. According to molecular models of the corresponding Michaelis complexes, the aryl moiety of Y337 is within interaction distance of the 1,2,2-trimethylpropyloxy group of both the $P_SC_S$- and $P_SC_R$-soman diastereomers (Figure 1A,B). Examination of phosphonylation kinetics of the Y337A HuAChE, for phosphonylation by the $P_SC_S$- and $P_SC_R$-soman diastereomers, shows 6−10-fold decreases in the bimolecular rate constants, yet there is no significant change in the stereoselectivity for the $P_SC_S$-isomer (3-fold) compared to that to the wild type HuAChE. Thus, replacement at position 337 of HuAChE seems to introduce about half of the moderate (6−8-fold) stereoselectivity for the $P_SC_S$-stereomer, characteristic of BChEs (see ref *20* and the data cited in Table 2).

*Effects of Replacements of Residues of the H-Bond Network on the Rates of Formation and Dealkylation of Diastereomeric $P_S$-Soman Conjugates with HuAChE Enzymes*. The H-bond network in the HuAChE active center was suggested to include the carboxylates of two of the three buried acidic residues (Glu202 and Glu450), the hydroxyl group of residue Tyr133, the backbone amide nitrogens of Gly122 and Gly448, and two water molecules corresponding to solvent molecules in the structure of TcAChE (*12*, *21*). The presence and positioning of these water molecules were recently corroborated by the reported structure of the HuAChE−fasciculin complex (*5*), further supporting the notion that such a network is one of the characteristic features of the AChE functional architecture. Replacement of each of the acidic residues (Glu202 and Glu450) affected the catalytic activity of the resulting enzymes toward both charged and noncharged substrates as well as toward phosphate inhibitors (*12*, *21*, *23*). This effect was attributed to reorganization of the active center upon replacement of the carboxylates with noncharged moieties, rather than to removal of negative charge from the vicinity of the catalytic Ser203.

Rate constants for phosphonylation by the $P_S$-soman diastereomers, of the H-bond network subsite HuAChE mutants (E202Q, E450A, and Y133F), indicate again the similarity in the reactivity phenotypes of the three enzymes (*12*, *21*, *23*). The decrease in reactivity toward the $P_SC_S$-soman is 52−125-fold, while the corresponding reactivity decrease toward the $P_SC_R$-soman is 240−890-fold (see Table 3). Interestingly, these effects were more pronounced than those precipitated by perturbations of the H-bond network, on reactivity toward certain phosphates (*12*). The larger decline in reactivity toward the $P_SC_R$-soman stereomer gives rise to a moderate stereoselectivity of these mutant enzymes toward the $P_SC_S$-stereomer (6−13-fold; see Table 3). We note that a similar stereoselectivity was recently reported for the E197Q human BChE (equivalent to E202Q in HuAChE) (*20*); however, while the wild type HuAChE is practically nonselective, with respect to $P_S$-soman diastereomers, the

Table 3: Effects of Mutation of Residues in the H-Bond Network and the Hydrophobic Pocket on the Rate Constants of Formation ($k_i$) and Aging ($k_a$) of $P_S$-Somanyl Conjugates

| | $k_{app}$[a] ($\times 10^8$ $min^{-1}$ $M^{-1}$) | phosphonylation $k_i$ (pH 8.0 and 24 °C) ($\times 10^4$ $min^{-1}$ $M^{-1}$) | | aging $k_a$ (pH 8.0 and 24 °C) ($\times 10^{-3}$ $min^{-1}$) | |
|---|---|---|---|---|---|
| | ATC | $P_SC_S$ | $P_SC_R$ | $P_SC_S$ | $P_SC_R$ |
| rHuAChE | 28.6 | 15000 ± 2600 | 8000 ± 400 | 130 ± 30 | 92 ± 25 |
| E202Q | 2.1 | 290 ± 40 | 33 ± 3 | 0.6 ± 0.1 | 0.24 ± 0.05 |
| E450A | 0.7 | 120 ± 50 | 9 ± 3 | 4.7 ± 0.8 | 1.2 ± 0.3 |
| Y133F | 4.2 | 140 ± 10 | 22 ± 6 | ND | ND |
| Y133A | 0.04 | 3.3 ± 0.8 | 0.46 ± 0.05 | 8 ± 2 | 3.8 ± 0.8 |
| F338A | 10.0 | 7000 ± 2400 | 2800 ± 500 | 0.8 ± 0.1 | 1.3 ± 0.3 |
| W86F | 2.6 | 2300 ± 500 | 600 ± 200 | 7.6 ± 1.5 | 3.0 ± 0.6 |
| W86A | 0.009 | 2300 ± 900 | 150 ± 40 | <0.06[b] | <0.06[b] |
| wild type BChE | 14.3 | 4000[c] | 500[c] | | |
| BChE-E197Q[b] | − | 500[c] | 23[c] | | |

[a] Ordentlich et al. (*6*). [b] The values for the $k_a$ constants for the W86A mutant at pH 7 are $0.34 \times 10^{-3}$ $min^{-1}$ for $C_SP_S$ and $\leq 0.3 \times 10^{-3}$ $min^{-1}$ for $C_RP_S$. [c] pH 7.5 and 25 °C (*20*).

wild type human BChE already shows a 8-fold selectivity toward the $P_SC_S$-soman (*20*).

Compared to other residue substitutions in the H-bond network, substitution of Tyr133 with alanine resulted in a very dramatic decrease in reactivity toward both the $P_SC_S$- and the $P_SC_R$-soman diastereomers (4550- and 17400-fold, respectively). Similar effects of this substitution were observed in the past on catalytic activity (see Table 3) and on reactivity toward the phosphate DFP and were explained by a steric blockage due to the altered conformation of Trp86 in the Y133A enzyme (*28*). Interestingly, despite the exceedingly low reactivities of the Y133A HuAChE toward the $P_S$-soman diastereomers, its stereoselectivity (7-fold) resembles those of other enzymes carrying replacements in the H-bond network.

Participation of the H-bond network residue Glu202 in the aging process of somanyl−HuAChE conjugates, as well as in the enzyme hydrolytic activity, seems to be strongly dependent on the exact location and orientation of its carboxylate (*21*, *23*, *24*). Other constituents of the network, residues Glu450 and Tyr133, participate in orienting the Glu202 carboxylate and therefore exert an indirect influence on the aging process (*23*). Yet, our earlier results (*23*) demonstrate that replacement of residue Glu202 with either noncharged (alanine and glutamine) or charged (aspartate) amino acids results in a similar and large reduction in the rate of aging, indicating that the contribution of Glu202 cannot be rationalized by simple electrostatic interactions with the evolving carbocation (*42*). The very limited stereospecificity (1−3-fold) of the aging process, observed for the $P_SC_S$-somanyl adducts of the wild type and the E202Q HuAChEs, does not seem to support the notion that a difference in the $C_\alpha$ positioning is of consequence for the dealkylation mechanism. Furthermore, similar stereospecificities (4- and 2-fold) are observed also for conjugates of E450A and Y133A, respectively (Table 3), suggesting that this minor effect may be common to the replacement of H-bond network residues and is not primarily related to specific interactions of the Glu202 carboxylate with the partially charged alkoxy moiety (see Scheme 2).

*Effect of Replacement of Residues of the Hydrophobic Pocket on the Rates of Formation and Dealkylation of Diastereomeric $P_S$-Soman Conjugates with HuAChE Enzymes*. The aromatic patch in the HuAChE active center consisting of residues Trp86, Tyr337, and Phe338 (*14*) defines a hydrophobic pocket for the alkoxy leaving groups of the substrates as well as for the phosphoryl alkoxy substituents of organophosphates such as DFP or DEFP (*6*, *12*). In a previous study, we found that replacement of residues Tyr337 and Phe338 had only a limited effect on reactivity toward racemic soman (*23*). Results of the present investigation are consistent with this finding, although the reactivity toward the $P_SC_R$-soman seems to be somewhat more affected than that toward the corresponding $P_SC_S$-isomer. Replacement of residue Trp86 with alanine or phenylalanine had a limited and equivalent effect on phosphonylation rates for phosphonylation by the $P_SC_S$-soman (7-fold), suggesting that the reduced reactivity did not result from the loss of specific interactions with the residue at position 86. Such a conclusion is consistent with molecular models of the corresponding Michaelis complexes which do not indicate interactions of residues at position 86 with the ligand $C_\alpha$-methyl substituent. In contrast, reactivities of both the W86F and W86A enzymes toward the $P_SC_R$-soman are considerably lower (13- and 53-fold, respectively, compared to that of the wild type enzyme), although for the two $P_S$-diastereomers, the orientation of the alkoxy group with respect to the hydrophobic pocket is rather similar.

Scheme 2

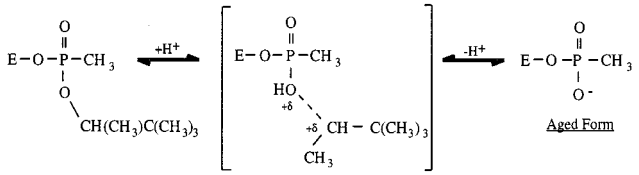


Molecular models suggest that the hydrophobic pocket does not interact with alkoxy substituents of the $P_R$-phosphonate diastereomers (Figures 1 and 3A). To test this suggestion, the reactivity of the W86F HuAChE toward the $P_RC_S$-soman has been evaluated. Indeed, the value of the corresponding phosphonylation rate constant ($0.2 \times 10^4$ $min^{-1}$ $M^{-1}$) is equal to that of the wild type enzyme. Due to such correspondence between model predictions and the experimental findings, and in view of the exceedingly large amount of enzyme required, further phosphonylations by the $P_R$-soman diastereomers were not carried out with hydrophobic pocket HuAChE mutants.

The crucial importance of residue Trp86, which constitutes the HuAChE choline binding site (*6*, *41*) and which is also

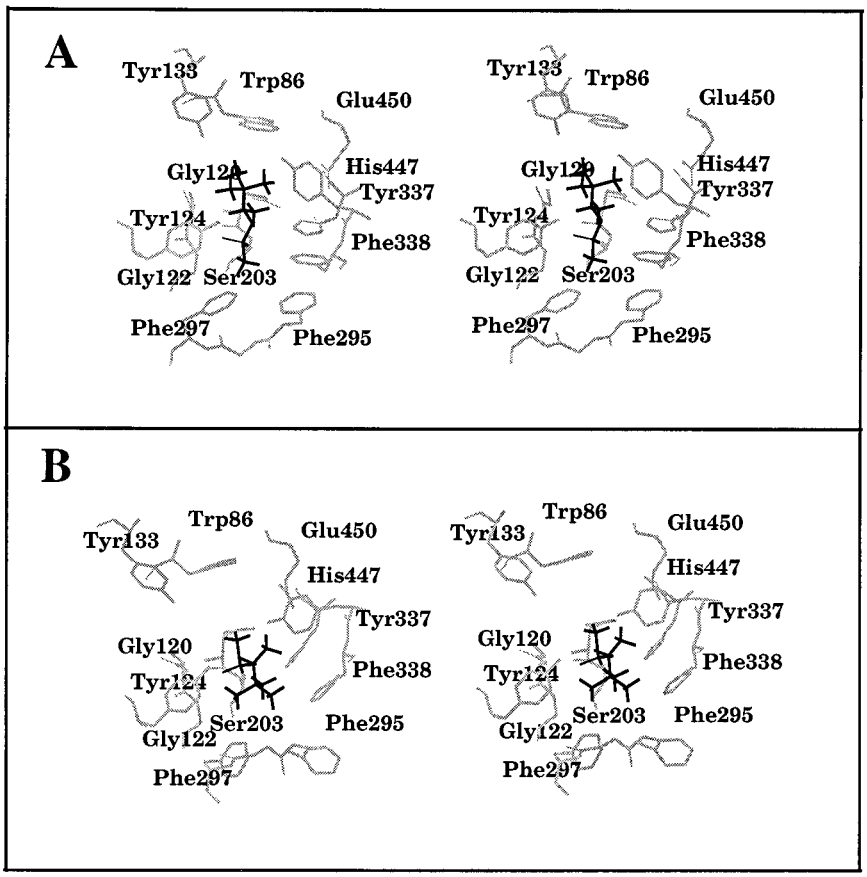


FIGURE 4: Covalent conjugates of the $P_SC_S$- and $P_RC_R$-soman−HuAChE conjugates (shown in stereoview). Only amino acids adjacent to the inhibitor are shown, and hydrogen atoms of the protein are omitted for clarity. The somanyl moieties are shown as heavy lines. (A) $P_SC_S$-somanyl conjugate. Note that the $C_\alpha$-methyl substituent is proximal to the aromatic moieties of residues Tyr337 and Phe338. (B) $P_RC_R$-somanyl conjugate. Note that the conformation of the acyl pocket main chain was modeled according to the recently resolved (*35*) X-ray structure of the aged DFP−TcAChE conjugate (see Materials and Methods), in which the acyl pocket is distorted compared to that of the inhibitor free enzyme.

part of the hydrophobic pocket, to the aging process of $P_S$-somanyl−HuAChE conjugates was already demonstrated by studies with the racemic phosphonate (*23*, *24*). Replacement of this residue by alanine resulted in a dramatic decrease (over $10^3$-fold) in the dealkylation rate. Such a role for Trp86 was hypothesized to involve the stabilization of partial positive charge on the $C_\beta$-methyl substituents, imparted through hyperconjugation with the evolving carbocation on the $C_\alpha$ (Scheme 2) of the alkoxy group, by cation−$\pi$ interactions (*23*, *24*). Due to this rate decrease, no dealkylation of the racemic conjugate could be detected for several days at pH 8; however, at a lower pH a slow reaction could be observed with a rate constant 1850-fold lower than the corresponding value for the wild type enzyme (*23*). In this investigation, we examined the possible contribution of the Trp86 residue to the stereospecificity of the dealkylation process, with respect to the alkoxy $C_\alpha$ chirality. Since as for the racemic conjugate, the kinetics of aging of $P_SC_S$- and the $P_SC_R$-somanyl−W86A HuAChEs could not be followed at pH 8, the respective rate constants at pH 7 were measured (see the footnote of Table 3). The values obtained ($0.34 \times 10^{-3}$ and $\leq 0.3 \times 10^{-3}$ $min^{-1}$, respectively; see the footnote of Table 3) are in good agreement with that obtained for the racemic conjugate ($0.2 \times 10^{-3}$ $min^{-1}$; *23*) and demonstrate that the effect of residue Trp86 does not depend on the chirality of the alkoxy moiety.

The contribution of residue Phe338 to the aging process of the somanyl−HuAChE conjugate was proposed to involve interaction with residue His447 rather then steric interference with the somanyl alkoxy moiety (*21*, *23*). According to molecular models, the $C_\alpha$-methyl substituent is closer to the phenyl moiety of Phe338 in the $P_SC_S$- than in the $P_SC_R$-conjugate (Figure 4A), and therefore if as recently suggested (*43*) steric effects are involved, replacement of this residue should have affected differently the rates of dealkylation of the corresponding somanyl−F338A HuAChE conjugates. The nearly equivalent values of the first-order rate constants of aging ($k_a$) observed for the diastereomeric $P_S$-somanyl−HuAChE conjugates adducts do not support this notion (see Table 3).

## DISCUSSION

*Determinants of Stereoselectivity of HuAChE Phosphonylation by Soman Stereomers.* Determination of the apparent bimolecular rate constants for HuAChE phosphonylation by the four stereomers of soman allowed us to obtain an accurate measure of the AChE stereoselectivity with respect to the phosphorus chirality in methyl phosphonofluoridates. In the past, only the upper limits of AChE reactivity toward the $P_R$-diastereomers of agents such as 2-propyl, 2-octyl, or 1,2,2-trimethylpropyl methylphosphonofluoridates could be found in the literature (*17*, *35*, *37*). The finding that phosphonylation by the $P_S$-soman diastereomers is almost $10^5$-fold faster than

that by the corresponding $P_R$-diastereomers signifies that the enzyme interacts very differently with the two soman diastereomeric pairs. These differences should be evident in the respective Michaelis complexes since their stabilities appear to determine the AChE reactivity characteristics toward organophosphorus inhibitors (*12*, *16*, *44*, *45*). In such complexes, the phosphorus atom should be proximal to the nucleophilic Ser203, and as recently shown (*13*), the P═O bond has to be polarized by interactions with the oxyanion hole. Therefore, the tight complementarity of the $P_S$-soman diastereomers with the HuAChE active center is bound to be influenced primarily by the accommodation of their alkoxy substituents. In addition, the juxtaposition of the P═O bond relative to the elements of the HuAChE catalytic machinery defines the orientation of the alkoxy substituent within the active center and can guide the docking of different soman stereomers. The HuAChE−soman molecular models allow us to define the different active center environments probed by the alkoxy groups of the $P_S$- and the $P_R$-soman diasteromers and seem to indicate that the low reactivities of the $P_R$-diastereomers arise mainly from steric constraints which prevent accommodation of the 1,2,2-trimethylpropyloxy group and practically exclude it from the acyl pocket (see Figures 1 and 3A). Such a notion is consistent with the observation that the difference in substrate specificity between AChE and BChE is predominantly due to the more open acyl pocket of the latter accommodating more readily the larger acyl group of butyrylcholine (*6*, *15*). It is also in agreement with the enhanced reactivity of phosphates DFP, DEFP, and paraoxon toward HuAChEs modified at the acyl pocket (*23*, *35*). The estimated nearly $10^4$-fold AChE stereoselectivitiy for the respective $P_S$-enantiomer of sarin is also compatible with this rationale since BChE is not stereoselective toward sarin enantiomers (*38*). These findings as well as the molecular models could suggest that, as proposed in the past (*28*, *41*, *46*), interactions of phosphonofluoridates such as soman or sarin with AChE and BChE reveal nearly equivalent architectures of the respective active centers, differing only in the void volume of the acyl pocket. Results of this study suggest that although this view is basically correct it is also somewhat simplistic since it does not account for some of the kinetic data, especially with respect to phosphonylation of HuAChE enzymes mutated at the acyl pocket, as discussed below.

BChE and the F295l/F297V HuAChE contain the same composition of the acyl pocket, and therefore could be expected to exhibit comparable stereoselectivities with respect to soman phosphorus chirality. Indeed, the observed stereoselectivity of the F295L/F297V HuAChE and of EqBChE, favoring the $P_SC_S$-soman over the $P_RC_S$-stereomer (330- and 500-fold, respectively; see Table 2) and the $P_SC_R$-soman over the $P_RC_R$-stereomer (33- and 6-fold, respectively), suggests that the AChE acyl pocket is the main determinant of the relative reactivity toward the $P_S$- and $P_R$-soman diastereomers. However, the actual reactivity profiles of the F295L/F297V HuAChE and EqBChE toward soman isomers are quite different. The phosphonylation rate constants of the double mutant, with the $P_RC_S$- and $P_RC_R$-diastereomers, are 5- and 22-fold higher, respectively, than the corresponding values for the wild type enzyme. Yet these constants are also 12- and 38-fold lower than the corresponding values for EqBChE. These comparisons imply that in the F295L/F297V enzyme, the accommodation of the $P_R$-soman alkoxy moieties is still inferior compared to that in BChE. Moreover, introduction of a BChE-like acyl pocket into HuAChE results in a surprising decrease in the reactivity toward the $P_SC_S$- and $P_SC_R$-soman diastereomers (45- and 53-fold, respectively). On the other hand, the reactivity of equine BChE toward these stereomers is 2.5- and 8-fold lower, respectively, than that of wild type HuAChE, demonstrating that the active center architecture probed by interaction of soman stereomers with the F295L/F297V HuAChE is different from that probed by these interactions with BChE.

Unlike the case of the double mutant, where partial accommodation of both the $P_R$-soman diastereomers is possibly due to a sufficient opening of the acyl pocket, replacement of residue Phe295 by a smaller amino acid, alanine, seems to enable the accommodation of the $P_RC_R$- but not of the $P_RC_S$-stereomer. This is suggested by the observation that the reactivity of the F295A enzyme toward the $P_RC_R$-soman resembles that of the F295L/F297V HuAChE, while its reactivity toward the $P_RC_S$-soman is practically equivalent to that of the wild type enzyme (see Table 2). Molecular models of the respective F295A enzyme Michaelis complexes are also consistent with this conclusion (compare Figure 1D to Figure 3C), indicating that the $P_RC_R$-soman can be accommodated in the acyl pocket and that its conformation resembles that in the corresponding complex of the F295V/F297L enzyme (not shown). Yet, in the model of the F295A−$P_RC_S$-soman noncovalent complex, the alkoxy moiety is mostly excluded from the acyl pocket, as in the respective complex with the wild type HuAChE (compare Figure 1C to Figure 3B).

The effect of substituting Phe297, the other element of the HuAChE acyl pocket, with alanine is more difficult to analyze since the reactivity of the F297A enzyme toward the $P_RC_R$-soman is merely 2.5-fold higher than that of the wild type enzyme. On the other hand, this enzyme appears to be 4-fold less reactive toward the $P_RC_S$-soman, suggesting that substitution at position 297 affects the acyl pocket structure in a manner different from that of an analogous substitution at position 295. Therefore, it seems that the 10-fold stereoselectivity of the F297A enzyme toward the $P_RC_R$- over the $P_RC_S$-soman may not originate from improved accommodation of the former stereomer in the acyl pocket. Such differential kinetic behavior of the F295A versus F297A was already observed in the past toward substrates such as butyrylthiocholine and organophosphates (*6*, *12*). It should be noted that molecular models of the respective Michaelis complexes seem to suggest that the modified acyl pockets of both the F295A (Figure 3B,C) and F297A enzymes should be open enough to relieve part of the steric strain due to accommodation of the soman alkoxy group.

The merely 2-fold stereoselectivity observed for the wild type HuAChE, with respect to the $P_SC_S$-stereomer, compared to that of the $P_SC_R$-isomer, implies that the $C_\alpha$-methyl substituent should be similarly accommodated in the respective Michaelis complexes. On the other hand, molecular models of these complexes suggest that the $C_\alpha$-methyl group of the $P_SC_S$-diastereomer is oriented toward the aromatic systems of the hydrophobic pocket residues Tyr337 and Phe338, while that of the $P_SC_R$-stereomer points away (compare Figure 1A to Figure 2B). Thus, substitution of either of these residues could have been expected to

selectively lower the reactivity toward the $P_SC_S$-stereomer. Indeed, the reactivities of both the Y337A and the F338A HuAChE enzymes toward the $P_SC_S$-stereomer are somewhat lower than that of the wild type enzyme; however, the reactivity toward the $P_SC_R$-stereomer is similarly affected. A more significant relative decrease in the reactivity toward the $P_S$-diastereomers is observed upon substitution by alanine of the third constituent of the hydrophobic pocket, residue Trp86, yet this decrease cannot be accounted for by molecular models of the corresponding Michaelis complex. The limited utility of the models, in these specific cases, may originate from shortcomings of the modeling methodology and/or may be due to their absolute dependence on the static crystallographic structures of AChEs. Since the dynamics of the induced fit probably taking place during Michaelis complex formation cannot be readily simulated in the model building procedure, the resulting models may not be accurate enough. Furthermore, as already suggested for the AChE noncovalent complexes with tacrine and huperzine A, the solid-state structures may not be identical to those in solution (*14*). The recently resolved structures of HuAChE and of its E202Q mutant share a nearly identical structure of the active center (*5*), yet the difference in the reactivity and stereoselectivity of the two enzymes toward soman stereomers is greater than could have been predicted from these X-ray structures.

*Significance of the Lack of Stereoselectivity in Aging of Soman−HuAChE Conjugates.* In this study, the diastereomeric $P_R$-somanyl−HuAChE conjugates proved to be stable for days without appreciable decomposition or aging. This absolute stereospecificity ($>1.5 \times 10^4$ for the stereomeric $P_SC_S$-somanyl−HuAChE conjugate as compared to that of the respective $P_RC_S$-conjugate) is consistent with most of the structural models of $P_R$-phosphonyl−AChE adducts (*15*, *23*, *34*) (see Figure 4B) as well as with the recently proposed involvement of specific ChE active center residues in the catalysis of the aging process (*23*, *24*, *43*). On the other hand, these results do not support the conclusion of a recent modeling study that the "dealkylation reaction is almost equally likely in all stereomers of soman-inhibited AChE" (*42*). The lack of dealkylation from the $P_R$-somanyl moiety suggests also that strain due to structural distortion of the adduct (*47*) is not the main driving force for this reaction. This conclusion is based on analogy to the recently disclosed preliminary three-dimensional structure of the DFP−TcAChE conjugate where the alkoxy substituent pointing toward the acyl pocket induces a marked deviation from the structure of the ligand-free enzyme (*35*).

Unlike the remarkable stereospecificity of the aging process with respect to the phosphorus chirality of the somanyl conjugates, the rates of aging for the $P_SC_S$- and $P_SC_R$-somanyl−HuAChE adducts were nearly equivalent, indicating that the asymmetric enzyme environment does not affect the rate-determining step of the dealkylation process. This was observed for enzymes mutated in the H-bond network as well as for those carrying replacements in the hydrophobic pocket. In particular, this is the case for replacements of Glu202 which participates directly in the aging process, or of residues Phe337 and Phe 338 which according to molecular models are proximal to the $C_\alpha$-methyl group in the $P_SC_S$-somanyl adduct, but not in the corresponding $P_SC_R$-conjugate. Such a lack of sensitivity to the immediate molecular environment of these $C_\alpha$-methyl substituents seems to be inconsistent with a possible mechanism of dealkylation through an anchimerically assisted elimination (a concerted elimination of the $C_\alpha$-hydroxy substituent and a 1,2-shift of a $C_\beta$-methyl group; see ref *48*), since such a process is bound to involve a formal inversion of the $C_\alpha$ configuration (*49*). During such an inversion process, the $C_\alpha$-methyl groups of the $C_S$- and the $C_R$-somanyl moieties should have sampled different chemical environments since the respective transition states of elimination are not equivalent, and therefore affect differentially the corresponding rates of dealkylation. On the other hand, the lack of $C_S$- or $C_R$-stereoselectivity in aging is compatible with a stepwise mechanism where formation of a carbocation precedes the 1,2-shift of a $C_\beta$-methyl group. In such a mechanism, the carbocations evolving from both the $P_SC_S$- and $P_SC_R$-somanyl moieties should be nearly equivalent with respect to the active center environment.

## ACKNOWLEDGMENT

We thank Dana Berman and Gali Sod-Moria for their excellent technical assistance and contribution.

## REFERENCES

1. Quinn, D. M. (1987) *Chem. Rev. 87*, 955−979.
2. Sussman, J. L., Harel, M., Frolow, F., Oefner, C., Goldman, A., Toker, L., and Silman, I. (1991) *Science 253*, 872−879.
3. Harel, M., Quinn, D. M., Nair, H. K., Silman, I., and Sussman, J. L. (1996) *J. Am. Chem. Soc. 118*, 2340−2346.
4. Raves, M. L., Harel, M., Pang, Y.-P., Silman, I., Kozikowski, A. P., and Sussman, J. L. (1997) *Nat. Struct. Biol. 4*, 57−63.
5. Kryger, G., Giles, K., Harel, M., Toker, L., Velan, B., Lazar, A., Kronman, C., Barak, D., Ariel, N., Shafferman, A., Silman, I., and Sussman, J. L. (1998) in *Structure and Function of Cholinesterases and Related Proteins* (Doctor, B. P., Quinn, D. M., Rotundo, R. L., and Taylor, P., Eds.) Plenum, London (in press).
6. Ordentlich, A., Barak, D., Kronman, C., Flashner, Y., Leitner, M., Segall, Y., Ariel, N., Cohen, S., Velan, B., and Shafferman, A. (1993) *J. Biol. Chem. 268*, 17083−17095.
7. Barak, D., Kronman, C., Ordentlich, A., Ariel, N., Bromberg, A., Marcus, D., Lazar, A., Velan, B., and Shafferman, A. (1994) *J. Biol. Chem. 264*, 6296−6305.
8. Shafferman, A., Kronman, C., Flashner, Y., Leitner, M., Grosfeld, H., Ordentlich, A., Gozes, Y., Cohen, S., Ariel, N., Barak, D., Harel, M., Silman, I., Sussman, J. L., and Velan, B. (1992) *J. Biol. Chem. 267*, 17640−17648.
9. Vellom, D. C., Radic, Z., Li, Y., Pickering, S. N., Camp, A., and Taylor, P. (1993) *Biochemistry 32*, 12−17.
10. Radic, Z., Gibney, G., Kawamoto, S., MacPhee-Quigley, K., Bongiorno, C., and Taylor, P. (1992) *Biochemistry 31*, 9760−9767.
11. Radic, Z., Pickering, N. A., Vellom, D. C., Camp, C., and Taylor, P. (1993) *Biochemistry 32*, 12074−12084.
12. Ordentlich, A., Barak, D., Kronman, C., Ariel, N., Segall, Y., Velan, B., and Shafferman, A. (1996) *J. Biol. Chem. 271*, 11953−11962.
13. Ordentlich, A., Barak, D., Kronman, C., Ariel, N., Segall, Y., Velan, B., and Shafferman, A. (1998) *J. Biol. Chem. 273*, 19509−19517.
14. Ariel, N., Ordentlich, A., Barak, D., Bino, T., Velan, B., and Shafferman, A. (1998) *Biochem. J. 335*, 95−102.
15. Hosea, N. A., Berman, H. A., and Taylor, P. (1995) *Biochemistry 34*, 11528−11536.
16. Berman, H. A., and Leonard, K. J. (1989) *J. Biol. Chem. 264*, 3942−3956.
17. Benschop, H. P., and De Jong, L. P. A. (1988) *Acc. Chem. Res. 21*, 368−374.

18. Keijer, J. H., and Wolring, G. Z. (1969) *Biochim. Biophys. Acta 185*, 465−468.
19. Benschop, H. P., Konings, C. A. G., Van Genderen, J., and De Jong, L. P. A. (1984) *Toxicol. Appl. Pharmacol. 72*, 61−74.
20. Millard, C. B., Lockridge, O., and Broomfield, C. A. (1998) *Biochemistry 37*, 237−247.
21. Ordentlich, A., Kronman, C., Barak, D., Stein, D., Ariel, N., Marcus, D., Velan, B., and Shafferman, A. (1993) *FEBS Lett. 334*, 215−220.
22. Hosea, N. A., Radic, Z., Tsigelny, I., Berman, H. A., Quinn, D. M., and Taylor, P. (1996) *Biochemistry 35*, 10995−11004.
23. Shafferman, A., Ordentlich, A., Barak, D., Stein, D., Ariel, N., and Velan, B. (1996) *Biochem. J. 318*, 833−840.
24. Barak, D., Ordentlich, A., Segall, Y., Velan, B., Benschop, H. P., De Jong, L. P. A., and Shafferman, A. (1997) *J. Am. Chem. Soc. 119*, 3157−3158.
25. Kronman, C., Velan, B., Gozes, Y., Leitner, M., Flashner, Y., Lazar, A., Marcus, D., Sery, T., Papier, A., Grosfeld, H., Cohen, S., and Shafferman, A. (1992) *Gene 121*, 295−304.
26. Velan, B., Grosfeld, H., Kronman, C., Leitner, M., Gozes, Y., Lazar, A., Flashner, Y., Markus, D., Cohen, S., and Shafferman, A. (1991) *J. Biol. Chem. 266*, 23977−23984.
27. Shafferman, A., Velan, B., Ordentlich, A., Kronman, C., Grosfeld, H., Leitner, M., Flashner, Y., Cohen, S., Barak, D., and Ariel, N. (1992) *EMBO J. 11*, 3561−3568.
28. Ordentlich, A., Barak, D., Kronman, C., Ariel, N., Segall, Y., Velan, B., and Shafferman, A. (1995) *J. Biol. Chem. 270*, 2082−2091.
29. Fischer, M., Ittah, A., Liefer, I., and Gorecki, M. (1993) *Mol. Cell. Neurobiol. 13*, 25−38.
30. Monard, C., and Quinchon, J. (1961) *Bull. Soc. Chim. Fr.*, 1084−1085.
31. Ellman, G. L., Courtney, K. D., Andres, V., and Featherstone, R. M. (1961) *Biochem. Pharmacol. 7*, 88−95.
32. Grosfeld, H., Barak, D., Ordentlich, A., Velan, B., and Shafferman, A. (1996) *Mol. Pharmacol. 50*, 639−649.
33. Barak, R., Ordentlich, A., Barak, D., Fischer, M., Hendrik, P., Benschop, H. P., De Jong, L. P. A., Velan, B., and Shafferman, A. (1997) *FEBS Lett. 407*, 347−352.
34. Barak, D., Ariel, N., Velan, B., and Shafferman, A. (1992) in *Multidiciplinary Approaches to Cholinesterase Functions* (Shafferman, A., and Velan, B., Eds.) pp 195−199, Plenum, London.
35. Millard, C. B., Kryger, G., Ordentlich, A., Harel, M., Raves, M. L., Greenblat, H., Segall, Y., Barak, D., Shafferman, A., Silman, I., and Sussman, J. L. (1998) in *Structure and Function of Cholinesterases and Related Proteins* (Doctor, B. P., Quinn, D. M., Rotundo, R. L., and Taylor, P., Eds.) Plenum, London (in press).
36. De Jong, L. P. A., and Benschop, H. P. (1988) in *Stereoselectivity of Pesticides: Biological and Chemical Problems* (Ariens, E. J., van Rensen, J. J. S., and Welling, W., Eds.) pp 109−149, Elsevier Science, Amsterdam.
37. Rauk, A., Shishkov, I. F., Vilkov, L. V., Koehler, K. F., and Kostyanovsky, R. G. (1995) *J. Am. Chem. Soc. 117*, 7180−7185.
38. Boter, H. L., De Jong, L. P. A., and Kienhuis, H. (1971) in *Interaction of Chemical Agents with Cholinergic Mechanisns*, pp 9−26, Israel Institute for Biological Research 16th Annual Biology Conference, Israel Institute for Biological Research, Ness-Ziona, Israel.
39. Viragh, C., Akhmetshin, R., and Kovach, I. M. (1997) *Biochemistry 36*, 8243−8252.
40. Michel, H. O., Hackley, B. E., Jr., Berkowitz, L., List, G., Hackley, E. B., Gilliam, W., and Paukan, M. (1967) *Arch. Biochem. Biophys. 121*, 29−34.
41. Harel, M., Sussman, J. L., Krejci, E., Bon, S., Chanal, P., Massoulie, J., and Silman, I. (1992) *Proc. Natl. Acad. Sci. U.S.A. 89*, 10827−10831.
42. Bencsura, A., Enyedy, I., and Kovach, I. M. (1995) *Biochemistry 34*, 8989−8999.
43. Masson, P., Fortier, P.-L., Albaret, C., Froment, M.-T., Bartels, C. F., and Lockridge, O. (1997) *Biochem. J. 327*, 601−607.
44. Berman, H. A. (1996) in *Enzymes of the Cholinesterase Family* (Quinn, D. M., Balasubramanian, A. S., Doctor, B. P., and Taylor, P., Eds.) pp 177−182, Plenum, New York and London.
45. Gray, P. J., and Dawson, R. M. (1987) *Toxicol. Appl. Pharmacol. 91*, 140−144.
46. Järv, J. (1984) *Bioorg. Chem. 12*, 259−278.
47. Cadogan, J. I. G., Eastlick, D., Hampson, F., and Mackie, R. K. (1969) *J. Chem. Soc. B*, 144−146.
48. Shubin, V. G. (1984) in *Contemporary Problems in Carbonium Ion Chemistry* (Rees, C., Ed.) Vol. 116/117, pp 267−342, Topics in Current Chemistry, Springer-Verlag, Berlin.
49. Kirmse, W. (1979) *Topics Curr. Chem. 80*, 125−311.
50. Massoulie, J., Sussman, J. L., Doctor, B. P., Soreq, H., Velan, B., Cygler, M., Rotundo, R., Shafferman, A., Silman, I., and Taylor, P. (1992) in *Multidisciplinary Approaches to Cholinesterase Functions* (Shafferman, A., and Velan, B., Eds.) pp 285−288, Plenum, London.
51. Bourne, N., and Williams, A. (1984) *J. Am. Chem. Soc. 106*, 7591−7596.

BI982261F